International Journal of Applied Engineering Research ISSN 0973-4562 Volume 12, Number 20 (2017) pp. 9679-9687

Land Surface Temperature Retrieval from LANDSAT data using Emissivity Estimation

Jeevalakshmi. D [1]
Research Scholar, Department of Electronics and Communication Engineering,
Sri Venkateswara University College of Engineering, Sri Venkateswara University,
Tirupati, Andhra Pradesh, India.
Orcid Id: 0000-0001-8647-9769

Dr. S. Narayana Reddy [2]
Professor, Department of Electronics and Communication Engineering,
Sri Venkateswara University College of Engineering, Sri Venkateswara University,
Tirupati, Andhra Pradesh, India.

Dr. B. Manikiam [3]
Sir MV - ISRO Chair Professor, Department of Physics,
Bangalore University, Jnanabharathi Campus,
Bangalore, Karnataka, India.

Abstract

Land surface temperature (LST) is an essential factor in many areas like global climate change studies, urban land use/land cover, geo-/biophysical and also a key input for climate models. LANDSAT 8, the latest satellite from LANDSAT series, has given lot of possibilities to study the land processes using remote sensing. In this study an attempt has been made to estimate LST over Chittoor district, Andhra Pradesh, India, using LANDSAT 8 – Operational Line Imager & Thermal Infrared Sensor (OLI & TIRS) satellite data. The variability of retrieved LSTs has been investigated with respect to Normalized Difference Vegetation Index (NDVI) values for different land use/land cover (LU/LC) types determined from the Landsat visible and NIR channels. The Land Surface Emissivity (LSE) values needed in order to apply the method have been estimated from a procedure that uses the visible and near infrared bands. The present study focuses on developing an ERDAS IMAGINE image processing method using the LANDSAT 8 thermal imagery of band 10 data. The difference between retrieved LST and Automatic Weather Station (AWS) data indicates that the technique works by giving an error of ±3^{o}C.

Keywords: Land Surface Temperature (LST), Land Surface Emissivity (LSE), Normalized Difference Vegetation Index (NDVI), Operational Line Imager & Thermal Infrared Sensor (OLI & TIRS), Remote sensing.

INTRODUCTION

Land Surface Temperature (LST) is the temperature of the surface which can be measured when the land surface is in direct contact to the measuring instrument. LST is nothing but the skin temperature of the land surface. Worldwide urbanization has significantly reshaped the landscape, which has important climatic implications across all scales due to the simultaneous transformation of natural land cover and introduction of urban materials i.e. anthropogenic surfaces. Identification and characterization of Urban Heat Island (UHI) is typically based on LST that varies spatially, due to the non-homogeneity of land surface cover and other atmospheric factors [1]. Ground surveys would permit a highly accurate Land Use Land Cover (LULC) classification, but they are time-consuming, burdensome and expensive, which highlights remote sensing an evident and preferred alternative. Medium spatial resolution data, such as that from the LANDSAT and SPOT are suitable for land cover or vegetation mapping at regional local scale. LANDSAT 8 carries two sensors, i.e., the Operational Land Imager (OLI) and the Thermal Infrared Sensor (TIRS). OLI collects data at a 30m spatial resolution with eight bands located in the visible and near-infrared and the shortwave infrared regions of the electromagnetic spectrum, and an additional panchromatic band of 15m spatial resolution. TIRS senses the TIR radiance at a spatial resolution of 100m using two bands located in the atmospheric window between 10 and 12 μm [2,3].

Various techniques have been developed to estimate LST for Urban Heat analysis, Meteorology and Climatology, Land Cover Dynamic monitoring using brightness temperature [1]; Split Window Technique and Single Channel Technique [2,4,5,6,7,8,9]. The technique used for the study area is developed in ERDAS IMAGINE 2016, with the model maker. The idea behind this technique was probably first suggested by Ugur Avdan et al., 2016 [10]. The technique presented in this paper is used for estimating the LST of a given LANDSAT 8 image with the input of the red band (0.64–

0.67μm), near infrared band (NIR) (0.85–0.88μm), and thermal infrared band10 (TIR) (10.60– 11.19μm). Following the instructions of USGS vide January 6, 2014, of not using TIRS band 11 due to its larger calibration unreliability, only band 10 was considered in the technique.

DESCRIPTION OF STUDY AREA AND DATA

Chittoor district is a part of Rayalaseema region of Andhra Pradesh. The district occupies an area of 15,359 square kilometers (5,930 sq mi). The district lies extreme south of the Andhra Pradesh state approximately between 12°37′ - 14°8′N and 78°3′ - 79°55′E (Lat/Long respectively). 30% of the total land is covered by forests in the district. The district constitutes of red loamy soil 57%, red sandy soil 34% and the remaining 9% is covered by black clay, black loamy, black sandy and red clay soils. Because of the higher altitude of the western parts compared to the eastern parts of the district, the temperature in the western parts, like Punganur, Madanapalle Horsley Hills are relatively lower than the eastern parts. The summer temperature reaches up to 46 °C in the eastern parts whereas in the western parts it ranges around 36° to 38 °C. Similarly the winter temperatures of the western parts are relatively in low range around 12 °C to 14 °C and in eastern parts it is about 16 °C to 18 °C. It receives an annual rainfall of 918.1 mm. The South West Monsoon and North East Monsoon are the prime sources of rainfall for the district [Source: Regional Agricultural Research Station].

The multispectral remote sensing images of Chittoor region of two dates were collected from USGS. Landsat 8 satellite images the entire earth once in 16 days. Band designations of Landsat8 are as given in Table 1 [11]. Satellite data over Chittoor region of 30th May and 21st October of 2015 (day time, level-1G product, path/row 143/51) have been used in this study. Satellite images of two dates of same region were downloaded from USGS website. The study area chosen includes water, bare soil, vegetation cover and built-up area. The images were resampled using nearest neighbor method. All the data are re-projected to a Universal Transverse Mercator (UTM) coordinate system, datum WGS84, zone 44.

METHODOLOGY

The approach to the proposed work to estimate LST is shown in the Figure 1. This technique can only be used to process LANDSAT 8 data. In this study, band 10 is used to estimate brightness temperature and bands 4 and 5 are used to calculate NDVI.

Table 1: Landsat 8 OLI and TIRS

Band Designations	Wavelength (μm)	Resolution (m)
Band 1 (Coastal Aerosol)	0.43 - 0.45	30
Band 2 (Blue)	0.45 - 0.51	30
Band 3 (Green)	0.53 - 0.59	30
Band 4 (Red)	0.64 - 0.67	30
Band 5 (Infrared)	0.85 - 0.88	30
Band 6 (Short wave infrared)	1.57 - 1.65	30
Band 7 (Short wave infrared)	2.11 - 2.29	30
Band 8 (Panchromatic)	0.50 - 0.68	15
Band 9 (Cirrus)	1.36 - 1.39	30
Band 10 (Thermal infrared)	10.6 - 11.19	100
Band 11 (Thermal infrared)	11.50 - 12.51	100

The steps involved in the proposed work are detailed in the following literature.

Step1:

The satellite data products were geometrically corrected data set. The metadata of the satellite images is presented in Table 2. The first step of the proposed work is to convert the DN (Digital Number) values of band10 to at-sensor spectral radiance using the following equation [11,12,13,14]

$$L_\lambda = \frac{(L_{max} - L_{min}) * Q_{cal}}{(Q_{calmax} - Q_{calmin})} + L_{min} - O_i \quad (1)$$

Where,

L_{max} is the maximum radiance ($Wm^{-2}sr^{-1}\mu m^{-1}$)

L_{min} is the minimum radiance ($Wm^{-2}sr^{-1}\mu m^{-1}$)

Q_{cal} is the DN value of pixel

Q_{calmax} is the maximum DN value of pixels

Q_{calmin} is the minimum DN value of pixels

O_i is the correction value for band 10

Step2:

After converting DN values to at- sensor spectral radiance, the TIRS band data should be converted to brightness temperature (BT) using the thermal constants given in metadata file and

Table 2: Metadata of the satellite image

Variable	Description	Value
K_1 K_2	Thermal constants, Band 10	774.8853 1321.0789
L_{max} L_{min}	Maximum and Minimum values of Radiance, Band 10	22.00180 0.10033
Q_{calmax} Q_{calmin}	Maximum and Minimum values of Quantize Calibration, Band 10	65535 1
O_i	Correction value, Band 10	0.29

the following equation

$$BT = \frac{K2}{\ln\left[\left(\frac{K_1}{L\lambda}\right)+1\right]} - 273.15 \quad (2)$$

Where K1 and K2 are the thermal constants of TIR band 10 which can be identified in the metadata file associated with the satellite image.

To have the results in Celsius, it is necessary to revise by adding absolute zero which is approximately equal to -273.15.

Since the atmosphere in our research area is comparitively dry and therefore, the range of water vapor values is relatively small, the atmospheric effect is not taken into consideration in retrieving the LST.

Step 3:

Normalized Difference Vegetation Index (NDVI) is essential to identify different land cover types of the study area. NDVI ranges between -1.0 to +1.0. NDVI is calculated on per-pixel basis as the normalized difference between the red band (0.64 - 0.67µm) and near infrared band (0.85-0.88µm) of the images using the formula.

$$NDVI = \frac{(NIR-RED)}{(NIR+RED)} \quad (3)$$

Where NIR is the near infrared band value of a pixel and RED is the red band value of the same pixel. Calculation of NDVI is necessary to further calculate proportional vegetation (Pv) and emissivity (ε).

Step 4:

Next step is to calculate proportional vegetation (P_v) from NDVI values obtained in step 3. This proportional vegetation gives the estimation of area under each land cover type. The vegetation and bare soil proportions are acquired from the NDVI of pure pixels. Values of NDVIv = 0.5 and NDVIs = 0.2 were proposed to apply in global conditions While the value for vegetated surfaces (NDVIv = 0.5) may be too low in some cases, for higher resolution data over agricultural sites, NDVIv can reach 0.8 or 0.9 [14]. P_v can be calculated using the equation (4).

$$P_v = \left(\frac{NDVI - NDVI_s}{NDVI_v - NDVI_s}\right)^2 \quad (4)$$

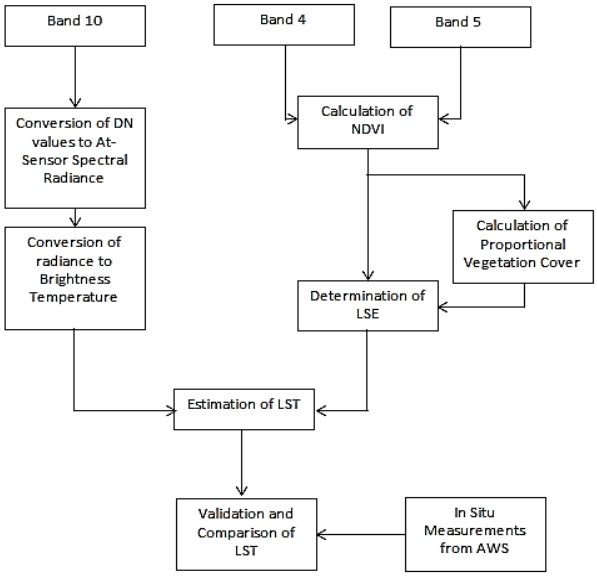

Figure 1: Flow diagram for LST retrieval

Step 5:

Calculation of land surface emissivity (LSE) is required to estimate LST since, LSE is a proportionality factor that scales the black body radiance (Plank's law) to measure emitted radiance and it is the ability of transmitting thermal energy across the surface into the atmosphere [10]. At the pixel scale, natural surfaces are heterogeneous in terms of variation in LSE. In addition, the LSE is largely dependent on the surface roughness, nature of vegetation cover etc.[15].

$$\varepsilon_\lambda = \varepsilon_{v\lambda} P_v + \varepsilon_{s\lambda} (1 - P_v) + C_\lambda \quad (5)$$

where ε_v and ε_s are the vegetation and soil emissivities respectively, and C is the surface roughness taken as a constant value of 0.005[16]. The emissivity of water bodies is utmost stable in comparison with land surfaces. Since the emissivity depends on the wavelength, the NDVI threshold method (NTM) [17] can be used to estimate the emissivity of different land surfaces in the 10-12 µm range.

$$\varepsilon_\lambda = \begin{cases} \varepsilon_{s\lambda}, & NDVI < NDVI_s \\ \varepsilon_{s\lambda} P_v + \varepsilon_{s\lambda}(1 - P_v) + C_\lambda, & NDVI_s \le NDVI \le NDVI_v \\ \varepsilon_{s\lambda} + c_\lambda, & NDVI > NDVI_v \end{cases} \quad (6)$$

The average emissivity of four major land cover types can be considered in Band 10 as, when the NDVI is less than 0, it is classified as water, and the emissivity value of 0.991 is given, for NDVI values between 0 and 0.2, it is considered that the land cover type is soil, and the emissivity value of 0.966 is assigned, values between 0.2 and 0.5 are considered as mixture of soil and vegetation cover and equation (6) is applied to calculate the emissivity. In the last case, when the NDVI value is greater than 0.5, it is considered as vegetation cover, and the value of 0.973 is assigned.

Step 6:

The final step is to calculate LST using brightness temperature (BT) of band 10 and LSE derived from Pv and NDVI [18]. LST can be retrieved using the equation (7)

$$T_s = \frac{BT}{\{1+[(\lambda BT/\rho)ln\varepsilon_\lambda]\}} \quad (7)$$

Where, T_s is the LST in Celsius (^{o} C), BT is at- sensor BT (^{o}C), λ is the average wavelength of band 10, ε_λ is the emissivity calculated from equation (6) and ρ is $(h \times \frac{c}{\sigma})$ which is equal to 1.438 x 10^{-2} mK in which, σ is the Boltzmann constant (1.38 x 10^{-23} J/K), h is Plank's constant (6.626 x 10^{-34}) and c is the velocity of light (3 x 10^8 m/s).

RESULTS

The study area Chittoor district, India, is shown in Figure 2. Satellite images of two dates of same region were downloaded from USGS website. The study area chosen includes water, bare soil, vegetation cover and built-up area. Landsat 8 data for the dates 30.05.2015 and 21.10.2015 (path/row: 143/51) were used for the present study. The Visible bands and Near Infrared bands are combined together to form a False Color Composite (FCC) image. The images were resampled using nearest neighbor method. All the data were re-projected to a Universal Transverse Mercator (UTM) coordinate system, datum WGS84, zone 44. The FCC images of two data sets are shown in Figure 3**.** The FCC images were created by layer stacking band 4, band 3 and band 2 of each data set correspondingly.

After conversion of DN values to spectral radiances, NDVI of each dataset is calculated. The NDVI images are shown in Figure 4. The NDVI values range between -1.0 to +1.0. An improvement in NDVI for vegetated land covers can be seen for the date 21.10.2015 when compared to the NDVI of 30.05.2015. That means, vegetation has been increased which shows an impact on the surface temperature. But, whereas, there is no much change in NDVI for the land cover types like built up area and bare land. LSE were estimated to retrieve LST for the acquired satellite data.

Since the atmosphere in our research area is comparitively dry and therefore, the range of water vapor values are relatively small. We are convinced with the results achieved and hence atmospheric effect is not taken into account in estimating the LST.

Automatic Weather Station (AWS) hourly data were collected from Andhra Pradesh State Development Planning Society (APSDPS), Andhra Pradesh, India and are used for comparison with the retrieved LST. The near surface air temperature of AWS is used for validating the retrieved LST of satellite images for 14 representative points.

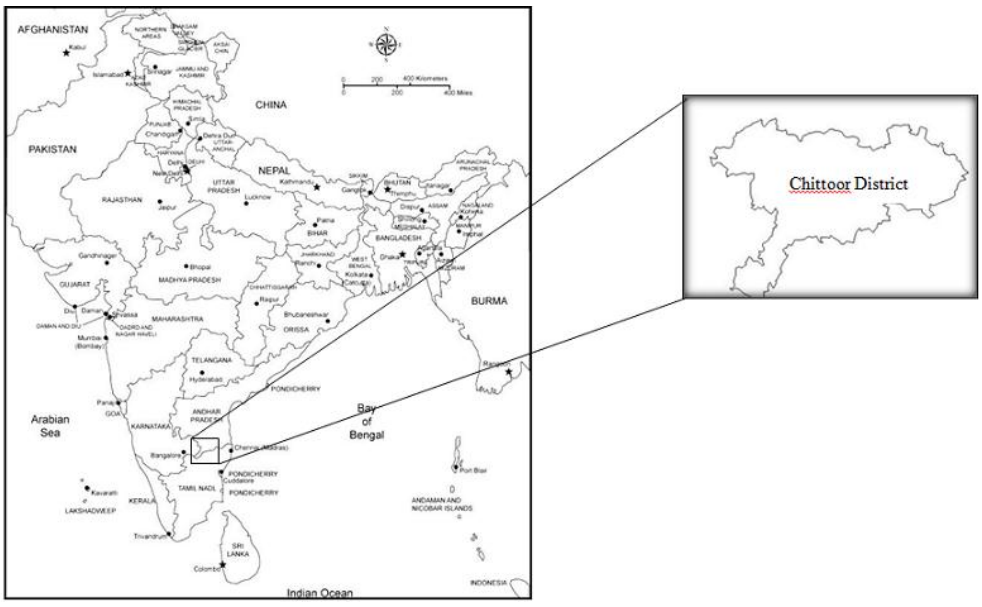

Figure 2: Geographic location of Chittoor District in India

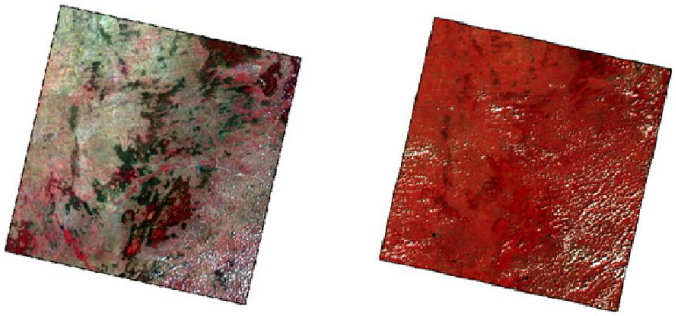

(a) (b)

Figure 3: FCC images of (a) 30.05.2015 and (b) 21.10.2015

The comparison was made with air temperature of AWS station, which is not same and can sometimes result in big differences since the resolution of LANDSAT 8 is 100m for the thermal band and 30m for the optical bands. The LST was calculated and taken for the pixel in which the AWS is located. The differences may also be due to some weather conditions and sensor characteristics of the AWS. And the other thing that has to be taken into consideration is the location of the thermal sensor in AWS which is at a height of 2 meters.

Comparison of retrieved LST and AWS surface air temperature

LSTs were retrieved for the downloaded satellite images using the mono window technique in ERDAS Imagine 2016. For the selected study area, 14 points were choosen in keeping view about the cloud pixels and other unwanted events for assessment of accuracy. The difference between retrieved LST and the AWS data for the two dates are shown in Table 3. The corresponding images of TIR band10 for both the datasets are shown in Figure 5. Plots showing AWS data and retrieved LST for the region of interest are shown in Figure 6. From the plots it can be observed that the retrieved LST and AWS data for the two datasets follows the same pattern for the selected 14 meteorological stations in the study area. LST maps of two datasets witht the meteorological stations and LST scale in ^{o}C are shown in Figure 7 and Figure 8 respectively.

Table 3: Retrieved LST and AWS data for 30.05.2015 and 21.10.2015

S.No.	Location	Latitude	Longitude	Land Cover types	30.05.2015				21.10.2015			
					NDVI	AWS Data at 5 A.M (^{o}C)	LST Retrieved (^{o}C)	Error (^{o}C)	NDVI	AWS Data at 5 A.M (^{o}C)	LST Retrieved (^{o}C)	Error (^{o}C)
1	Puttur	13.443777	79.556068	Built up	0.119	28.2	25.58	2.62	0.108	25.53	25.4	0.13
2	Chowdepalle	13.434461	78.692558	Bare land	0.042	24.41	26.83	-2.42	0.003	23.96	24.52	-0.56
3	Gudipala	13.078956	79.125069	Dense vegetation	0.335	23.52	21.64	1.88	0.529	23.01	24.5	-1.49
4	Aranyakandriga	13.402667	79.63726	Dense vegetation	0.305	27.18	25.67	1.51	0.574	24.63	25.83	-1.2
5	Nindra	13.376643	79.699702	Vegetation	0.261	28.53	30.68	-2.15	0.457	24.25	25.24	-0.99
6	Thavanampalle	13.262898	79.012993	Vegetation	0.046	22.95	23.54	-0.59	0.215	22.06	24.9	-2.84
7	Vijayapuram	13.267402	79.698624	Vegetation	0.346	25.46	27.82	-2.36	0.429	23.6	23.41	0.19
8	Yerpedu	13.693141	79.593695	Built up	-0.045	29.46	30.96	-1.5	0.05	24.78	27.66	-2.88
9	KVB Puram	13.53205	79.73996	Vegetation	0.044	31.23	31.94	-0.71	0.242	24.89	25.65	-0.76
10	Shivaramapuram	13.430556	78.409444	Vegetation	0.146	24.06	25.15	-1.09	0.377	21.18	22.49	-1.31
11	Tirupati	13.6175	79.403333	Built up	0.153	30.07	27.62	2.45	0.191	27.04	28.53	-1.49
12	Etavakili	13.374444	78.526667	Built up	0.015	21.15	23.74	-2.59	0.093	21.55	24.01	-2.46
13	Bandapalli	13.307083	79.121117	Bare land	0.105	25.98	26.17	-0.19	0.1	22.19	21.6	0.59
14	Sathravada	13.32085	79.542483	Vegetation	0.163	25.27	26.82	-1.55	0.215	25.01	26.03	-1.02

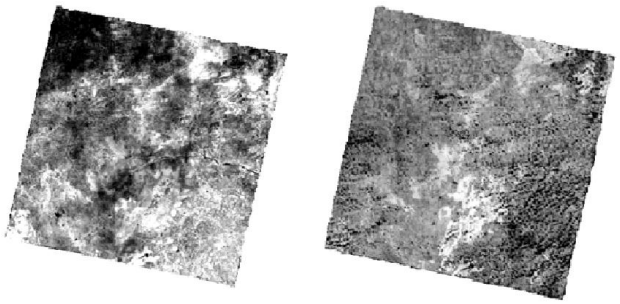

(a) (b)

Figure 4: NDVI images for (a) 30.05.2015 and (b) 21.10.2015

Conclusions & Future Scope

The model created in ERDAS Imagine 2016, estimated the LST for the selected datasets over the study area. The algorithm was created using the brightness temperature of TIRS band 10 and emissivity of different land covers types, derived from visible and near infrared bands of LANDSAT 8. The retrieved LSTs were verified using the near surface temperature of AWS data. From the comparison, it has been concluded based on the 14 meteorological stations that the standard deviation calculated for the first case was 1.79ºC and that for the second case it was 1.02ºC. The presented technique estimated LST with a smallest absolute difference of 0.19ºC and 0.56ºC for the two datasets respectively. These differences can be due to the difference between the resolutions of thermal band 10, which is of 100m and visible & NIR bands, which are of 30m. And also the comparison was done between the point measurement (AWS data) that is 2m above the surface and surface temperature (retrieved LST). This paper proposes an ERDAS image processing method to estimate LST and can be used to understand the urban development impacts on environment. This tool has proved as a dynamic tool to estimate LST using brightness temperature information of TIR sensor and Land surface emissivity (LSE) from proportional vegetation cover of optical bands of OLI sensor of LANDSAT 8.

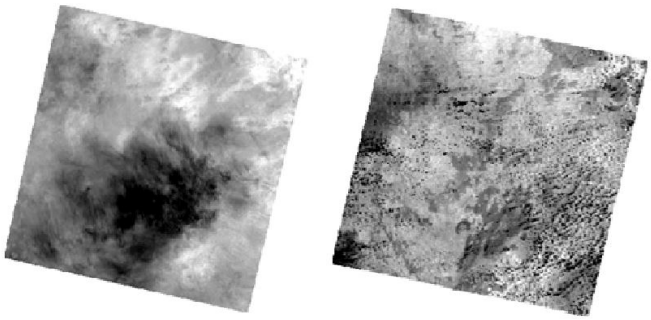

(a) (b)

Figure 5: TIR band 10 images for (a) 30.05.2015 and (b) 21.10.2015

In future studies, the technique to estimate LST can be altered by considering atmospheric effect and weather conditions of seasonal variations by processing the time series data over our region of interest. And also correlation between NDVI and LST can be demonstrated which helps specifically in urban heat analysis.

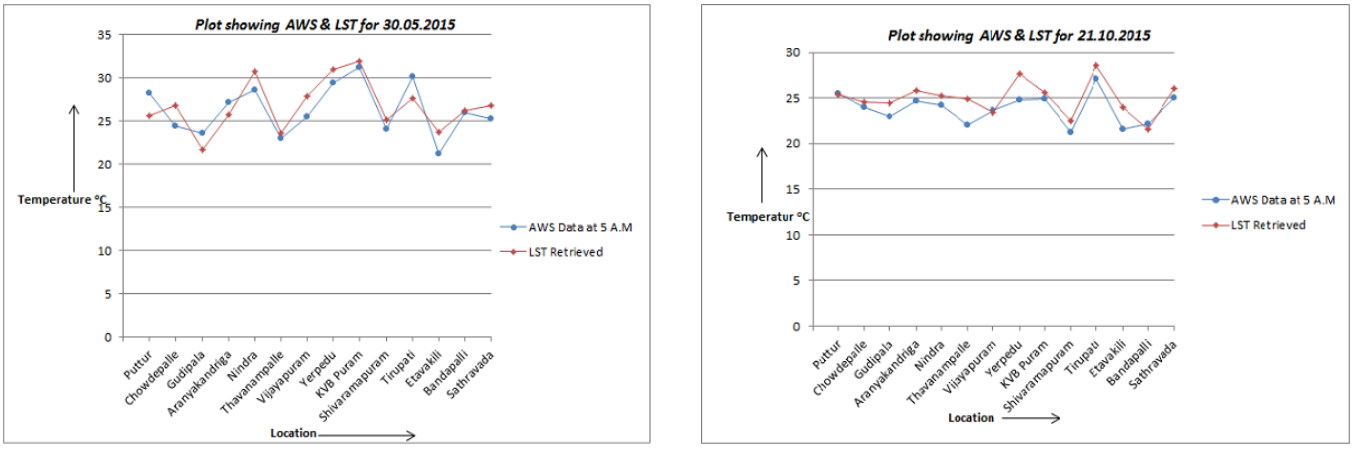

(a) (b)

Figure 6: Plots showing AWS & LST for (a) 30.05.2015 and (b) 21.10.2015

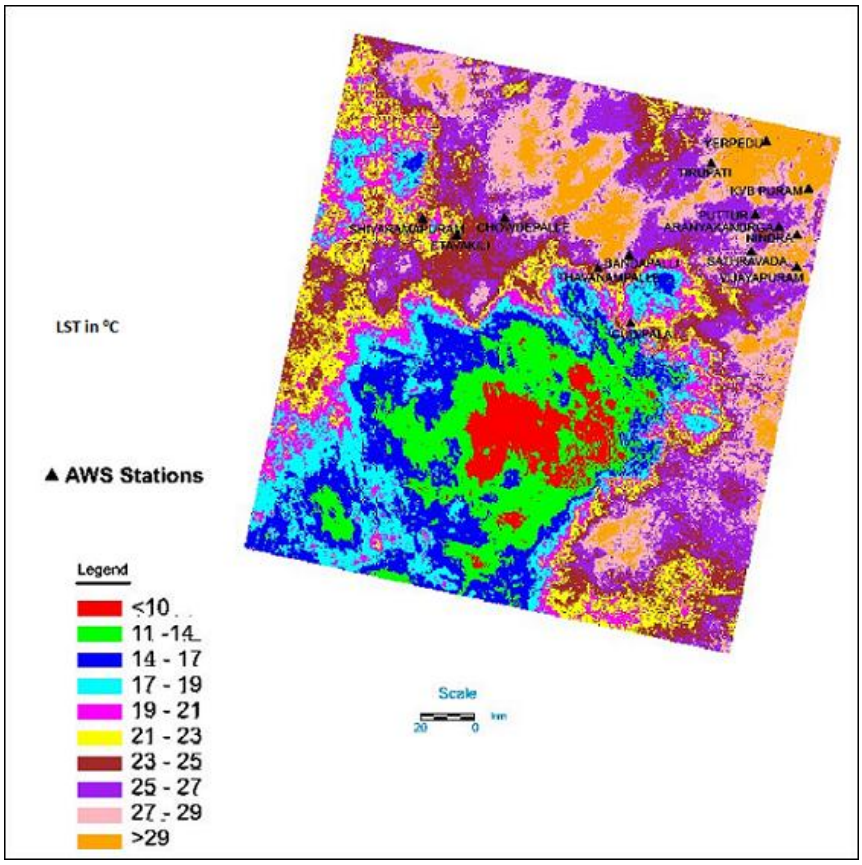

Figure: 7 LST map for 30.05.2015

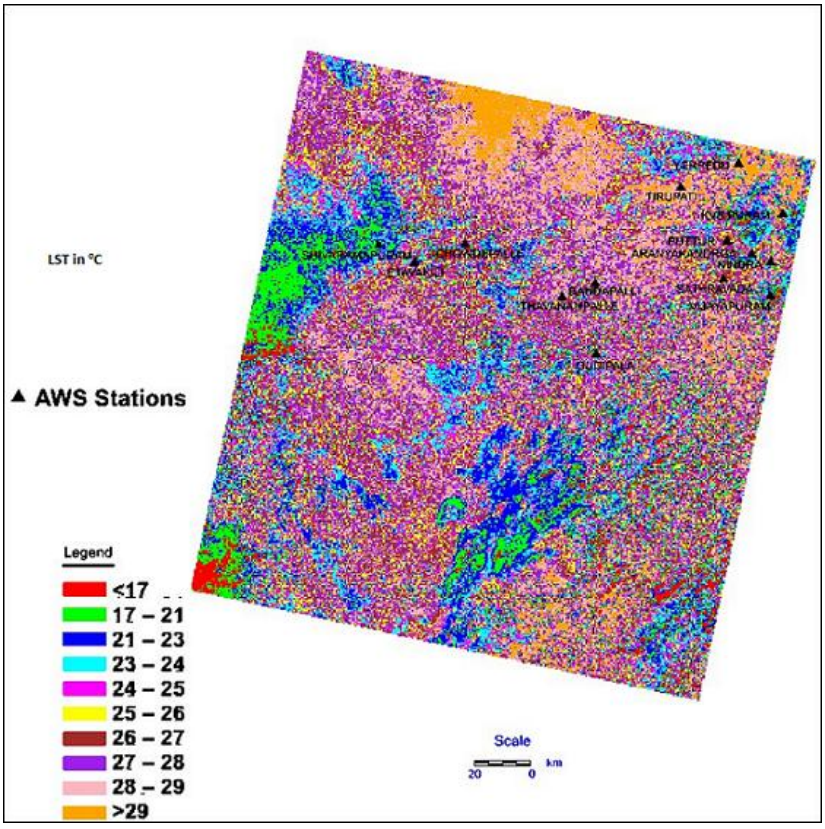

Figure 8: LST map for 21.10.2015

ACKNOWLEDGEMENT

The authors are extremely grateful to the Centre of Excellence on "Atmospheric Remote Sensing and Advanced Signal Processing", at Department of ECE, S V University College of Engineering, Tirupati, Andhra Pradesh, India, for providing necessary resources to carry out the present work. The LANDSAT 8 data from US Geological Survey (USGS), the AWS data from Andhra Pradesh State Development Planning Society (APSDPS) are acknowledged in this research.

REFERENCES

[1] Janak P. Joshi and Bindu Bhatt. "Estimating Temporal Land Surface Temperature Using Remote Sensing: A Study of Vadodara Urban Area, Gujarat", *International Journal of Geology, Earth and Environmental Sciences*, ISSN: 2277-2081, **Vol. 2(1)**, pp. 123-130, 2012.

[2] Juan C. Jiménez-Muñoz, José A. Sobrino, Dražen Skokovi´c, Cristian Mattar, & Jordi Cristóbal. "Land Surface Temperature Retrieval Methods from Landsat-8 Thermal Infrared Sensor Data", *IEEE Geoscience And Remote Sensing Letters*, **Vol. 11, No. 10,** pp. 1840- 1843, 2014.

[3] Charlie J. Tomlinson, Lee Chapman, John E. Thornes, & Christopher Baker. "Remote Sensing Land Surface Temperature for Meteorology and Climatology: A Review", Meteorological Applications, 18: 296–306, Doi: 10.1002/met.287, 2011.

[4] Qinqin Sun, Jianjun Tan, & Yonghang Xu. "An ERDAS image processing method for retrieving LST and describing urban heat evolution: a case study in the Pearl River Delta Region in South China", Environ Earth Sci., DOI 10.1007/s12665-009-0096-3, 59: 1047- 1055, 2010.

[5] Juan-Carlos Jiménez-Muñoz, & José A. Sobrino. "Split-Window Coefficients for Land Surface Temperature Retrieval from Low-Resolution Thermal Infrared Sensors", IEEE Geoscience and Remote Sensing Letters, Vol. 5, No. 4, pp.806- 809, 2008.

[6] Rajeshwari A, & Mani N D. "Estimation of Land Surface Temperature of Dindigul District Using Landsat 8 Data", International Journal of Research in Engineering and Technology, Vol.3 No.5, 2014.

[7] Xiaolei Yu, Xulin Guo, & Zhaocong Wu. "Land Surface Temperature Retrieval from Landsat 8 TIRS—Comparison between Radiative Transfer Equation-Based Method, Split Window Algorithm and Single Channel Method", Remote Sens., 6, 9829-9852; doi: 10.3390/ rs6109829, ISSN 2072- 4292, 2014.

[8] Meijun Jin, Junming Li, Caili Wang, & Ruilan Shang. "A Practical Split-Window Algorithm for Retrieving Land Surface Temperature from Landsat-8 Data and a Case Study of an Urban Area in China", Remote Sens., 7, 4371- 4390; doi: 10.3390/ rs70404371, ISSN 2072 – 4292, 2015.

[9] Offer Rozenstei, Zhihao Qin, Yevgeny Derimian, & Arnon Karnieli. "Derivation of Land Surface Temperature for Landsat-8 TIRS Using a Split Window Algorithm", Sensors, 14, 5768-5780; doi:10.3390/s140405768, ISSN 1424 – 8220, 2014.

[10] Ugur Avdan and Gordana Jovanovska. "Automated Mapping of Land Surface Temperature Using LANDSAT 8 Satellite Data", Journal of Sensors, Vol. 2016, Article ID 1480307, 2016.

[11] D. Jeevalakshmi, S. Narayana Reddy, & B. Manikiam. "Land cover classification based on NDVI using LANDSAT8 time series: A case study Tirupati region", IEEE International Conference on Communication and Signal Processing (ICCSP), pp.1332-1335,doi:0.1109/ICCSP.2016.7754369, 2016.

[12] Ren Zhibin & Zheng Haifeng & He Xingyuan & Zhang Dan & Yu Xingyang. "Estimation of the Relationship between Urban Vegetation Configuration and Land Surface Temperature with Remote Sensing", Journal of the Indian Society of Remote Sensing, 43(1):89–100, Doi 10.1007/s12524-014-0373-9, 2015.

[13] Julia A. Barsi, John R. Schott, Simon J. Hook, Nina G. Raqueno, Brian L. Markham and Robert G. Radocinski. "Landsat-8 Thermal Infrared Sensor (TIRS) Vicarious Radiometric Calibration", Remote Sensing, Vol.6, No. 11, pp. 11607- 11626, 2014.

[14] F. Wang, Z. Qin, C. Song, L. Tu, A. Karnieli, and S. Zhao. "An improved mono-window algorithm for land surface temperature retrieval from Landsat 8 thermal infrared sensor data," Remote Sensing, Vol. 7, no. 4, pp. 4268 – 4289, 2015.

[15] Javed Mallick, Yogesh Kant, & B.D.Bharath. "Estimation of Land Surface Temperature over Delhi Using Landsat-7 ETM+", J. Ind. Geophys. Union, Vol.12, No.3, pp.131-140, 2008.

[16] J. A. Sobrino and N. Raissouni. "Toward Remote Sensing Methods For Land Cover Dynamic Monitoring: Application to Morocco," International Journal of Remote Sensing, Vol. 21, No. 2, pp. 353 – 366, 2010.

[17] Jose A. Sobrino, Juan C. Jimenez-Munoz, Guillem Sòria, Mireia Romaguera, Luis Guanter, Antonio Plaza, & Pablo Martínez."Land Surface Emissivity Retrieval from Different VNIR and TIR Sensors", IEEE Transactions on Geoscience and Remote Sensing, Vol.46, No.2, pp.316 – 327, 2008.

[18] M. Stathopoulou, & C. Cartalis. "Daytime urban heat islands from Landsat ETM+ and Corine land cover data: An application to major cities in Greece", Solar Energy, Vol. 81, no. 3, pp. 358 – 368, 2007.

[19] F. Sattari and M. Hashim. "A Brief Review of Land Surface Temperature Retrieval Methods from Thermal Satellite Sensors", Middle-East Journal of Scientific Research 22 (5): 757-768, ISSN 1990 – 9233, 2014.

[20] USGS,http://landsat.usgs.gov/Landsat8_ Using_Product.php, 2013.